Marine Geology 259 (2009) 73–85

Contents lists available at ScienceDirect

Marine Geology

journal homepage: www.elsevier.com/locate/margeo

Seasonal patterns of coarse sediment transport on a mixed sand and gravel beach due to vessel wakes, wind waves, and tidal currents

Gregory M. Curtiss [a,*], Philip D. Osborne [b,1], Alexander R. Horner-Devine [a]

[a] University of Washington, United States
[b] Pacific International Engineering, PLLC, United States

ARTICLE INFO

Article history:
Received 13 October 2008
Received in revised form 5 December 2008
Accepted 29 December 2008

Keywords:
mixed sand and gravel beach
ferry wake wash
beach morphology
gravel transport
gravel tracers
RFID

ABSTRACT

Direct measurements of coarse sediment (gravel) transport are presented and analyzed from a mixed sand and gravel beach on Bainbridge Island, Puget Sound, WA that is exposed to wind waves, vessel wakes, and tidal currents in order to quantify the relative role of different forcing mechanisms and the corresponding time scales of morphological response. Radio Frequency Identification (RFID) Passive Integrated Transponder (PIT) technology is implemented in two coincident yearlong tracking studies of sediment particles, and complemented with beach profile surveys and meteorological and hydrodynamic measurements. The sampling of the gravel tracers provides sufficient resolution to reveal the dominant seasonal transport patterns, which include a range of wave climates. During winter storms, the predominant transport is due to wind waves in an alongshore uni-directional process, whereas tides and wakes play a relatively minor role. In non-storm intervals, transport is brought about by the combination of vessel wakes and tidal currents. Although tidal currents are not sufficient to initiate sediment movement alone, the combination of tidal currents and vessel wakes generate significant transport and provide a mechanism for post-storm recovery, re-distributing sediment onshore. Morphologic response occurs as a seasonal fluctuation of the upper beach profile from steep to flat and in sediment composition from gravel to coarse sand between non-storm and storm conditions respectively. These results, which are unique in their duration, suggest that mixed sand and gravel beaches experience different modes of behavior over the range of forcing conditions observed during a typical year. They point to the need for including grain composition in modeling mixed sand and gravel beach response and the need for long term observations of both forcing and response.

1. Introduction

Accurate predictions of sediment transport patterns and beach response are crucial for making well-informed decisions regarding coastal zone management. Advancement of predictive models requires high quality field and lab investigations for a range of forcing conditions and varying space and time scales. The majority of nearshore sediment transport research has been focused on beaches with a unimodal size distribution of either sand or gravel. The more complex situation of a mixed distribution of sand and gravel is less well studied. Our understanding of the seasonal and longer-term dynamics of mixed sand and gravel (MSG) beaches is limited by the lack of long term data of beach response and forcing and the limited predictive capability of numerical models. Mason and Coates (2001) identified hydraulic conductivity, infiltration and groundwater, wave reflection, and threshold of motion as the significant factors for sediment transport on MSG beaches which are not adequately included in any physically-based model. The few coarse-grained models that have been developed do not incorporate these processes and require field calibration (Van Wellen et al., 2000). Improvement and wider application of these models is limited by the lack of long term field data on MSG beaches to test model predictions of sediment transport and morphology.

Mixed sand and gravel (MSG) beaches occur mostly at high latitudes including on low energy, fetch restricted coasts such as the Puget Sound region (Finlayson, 2006), Tierra del Fuego (Isla, 1993), and the Marlborough Sounds, NZ (McDonald, 2003) and on open coasts in Great Britain (Mason et al., 1997) and New Zealand (Kirk, 1980; Ivamy and Kench, 2006), for example. Sediment on MSG beaches range over three orders of magnitude from coarse sand to pebble: 0.5φ to −6φ (Jennings and Schulmeister, 2002). The profile slopes are more gentle than gravel beaches and steeper than sand beaches, ranging from 5°–12° (Kirk, 1975).

Our current understanding of coarse sediment transport and morphology on MSG beaches is based primarily on short term field and laboratory studies, which encompass a limited range of wave

* Corresponding author. Golder Associates, Inc., Redmond, WA, United States. Tel.: +1 425 883 0777.
E-mail address: gcurtiss@golder.com (G.M. Curtiss).
[1] Present address: Golder Associates, Inc., Redmond, WA, United States.

0025-3227/$ – see front matter © 2009 Elsevier B.V. All rights reserved.
doi:10.1016/j.margeo.2008.12.009

climates. Sediment transport on MSG beaches is dominated by a concentration of energy in the swash zone (Kirk, 1975, 1980; Ivamy and Kench 2006; Buscombe and Masselink, 2006). Swash mechanics are controlled by the beach slope, differing infiltration rates caused by a groundwater table falling and rising with the tides, and the beach hydraulic conductivity, which depends strongly on grain size (Kulkarni et al., 2004). A sand and gravel mixture containing just 20% sand will have a hydraulic conductivity reduced by an order of magnitude over that of a pure gravel beach (Mason et al., 1997). Lab experiments by Quick and Dyksterhuis (1994) using a sand and gravel mixture confirmed that the sand fraction controls the beach permeability and, thus, the equilibrium slope through an increased offshore movement of material during high wave attack. More studies of this type are needed, including a broader range of grain size distributions and wave forcing. A threshold of motion is generally used in physically-based models to predict when individual sediment grains will become entrained by a fluid. In laboratory tests, Kuehnle (1993), Lopez de San Roman and Holmes (2002) and Wilcock and Crowe (2003) measured decreased mobility of gravel-sized particles on a MSG bed, motivating the need for including a mobility factor in physically-based models.

Observations have been made on MSG beaches on open coasts and in low energy, fetch-restricted environments. In the fetch-restricted case, few datasets exist for beaches where multiple process mechanisms (e.g. vessel wakes, wind waves, tides and tidal currents) are at work. Nordstrom and Jackson (1993) provide a conceptual model for low-energy MSG beaches in which more energetic waves move sediment offshore and less energetic waves move sediment onshore. Similarly, Dawe (2006) observed that the beach slope in the swash zone tends to be steeper during low energy waves and reduced during higher energy waves on a fetch-restricted MSG lakeshore in New Zealand. Wakes from vessels can also make a significant contribution to the wave climate in fetch-restricted environments (Abbe et al., 1991) and can impose new enduring beach profiles (Parnell and Kofoed-Hansen, 2001). In some areas of Puget Sound, in particular, MSG beaches and shorelines have exhibited sensitivity to changes in wake wave climate (Osborne et al., 2007). So far wakes have not been included in modeling approaches for MSG beach response. Beaches have shown variable response to wakes depending on several factors including vessel wake characteristics and sediment grain size composition (Kirkegaard et al., 1998; Osborne and Boak, 1999; Burke, 2003; McDonald, 2003; Osborne et al., 2007; Parnell et al., 2007).

Two relevant studies have observed the importance of vessel wakes on transport on MSG beaches. Osborne and Boak (1999) quantified the relative influence of vessel wakes and wind waves on long term morphology on a mixed sand and shell hash beach in New Zealand. Using combined wave measurements and suspended sediment concentrations they determined that the groupiness and nonlinearity of the vessel wakes had a greater potential to transport sediment than wind waves. However, the study was not able to identify the role of wakes in net alongshore or cross-shore transport or non-equilibrium beach response. Burke (2003) used magnetic tracers to determine alongshore and cross-shore transport on a gravel beach was the result of vessel wakes. The influence of storms was minimal and the longest observational period during the study was two weeks. Thus, the study was limited both in its ability to quantify response to strong wind wave forcing and to link morphologic changes to sediment transport. More work is needed to understand and accurately predict sediment transport and related morphologic changes on MSG beaches under multiple forcing mechanisms.

Our study provides long term direct measurements of gravel transport and beach response and identifies the relative influence of multiple forcing mechanisms on a MSG beach in a low-energy fetch restricted environment. Our study site, Point White, is located along Rich Passage in Puget Sound, WA, USA. The operation of ferries in the coastal system has provided the unique opportunity to study the dynamics of a MSG beach exposed to a wide range of wakes, wind waves, and tidal currents. During previous passenger only fast ferry (POFF) operations from 1999 to 2002 the upper foreshore of beaches in Rich Passage were eroded and the slopes were reduced. It is hypothesized that the longer period POFF wakes caused the flattening and erosion of the upper foreshore, whereas car ferries have resulted in beach steepening and accretion of the foreshore.

In this study, we obtain direct measurements of gravel transport using particle tracking and use profile measurements to record the morphological changes to the beach. Thus, sand transport is not directly measured but is reflected in the profile measurements. The contributions of wind waves, vessel wakes, and tidal currents are measured to evaluate seasonal patterns of transport and morphology at the site. In particular we address how these forcings control cross-shore and alongshore variations in the magnitude and direction of sediment transport.

2. Regional setting

The study site (Fig. 1) is an approximately 500 m length of MSG beach in Puget Sound on the east shore of Point White, at the southern end of Bainbridge Island, Washington, USA. Point White lies at the western end of Rich Passage, a narrow channel that provides the most direct vessel route between downtown Seattle and the city of Bremerton, WA. The beaches are backed by bulkheads and revetments of varying type and condition. Data were collected at two separate sites which are denoted here as PWA and PWB.

Beach and inter-tidal deposits at Point White are a thin layer of sediment eroded into a beach platform composed of Holocene age Vashon till (Haugerud, 2005). The mobile sediment layer is the result of reworking of coastal exposures of till, outwash sediments, and glaciomarine and glaciolacustrine deposits (Finlayson, 2006). The beach foreshore along Point White is generally steep (1:5 to 1:7), with a 20 to 30 m wide strip of beach gravel (pebble and cobble) overlying mixed sand and gravel. The beach unconsolidated layer varies in thickness from a few cm up to 2 m in places on the upper foreshore and at the toe of bulkheads. The unconsolidated gravel layer varies from 0.5 m to as thin as a single grain thickness of gravel armor on the lower foreshore. A unique feature of the beach is the median size of the gravel, which increases with decreasing elevation on the beach as also observed by Nordstrom and Jackson (1993) on a low energy estuarine beach. The cross-shore sorting is related to the relationship between swash energy, tide, and gravity/slope effects. The sediments were characterized by pebble counts of the surface layer and sieving samples from the upper 30 cm. The median grain size based on the pebble count is 22.5 mm at PWA and 17.0 mm at PWB. The median grain size for the entire sediment mixture based on sieving is 16.0 mm at PWA and 11.0 mm at PWB.

Multiple forcing mechanisms for sediment transport are present in Rich Passage. A wide range of tides and tidal currents exist, as well as seasonally variable winds that generate waves, and a variety of vessels operate that generate wakes. Tides in Puget Sound are mixed semi-diurnal with a meso- to macro-tidal range. Based on 12 yr of water level data from NOAA monitoring station 9447130 at Seattle, the average high tide is 3.5 m, above mean lower low water (mllw) and the highest daily high tide may reach 4.4 m, mllw. The combination of bathymetry in Rich Passage and the large tidal range generate flood and ebb currents up to 3.0 m/s in the main channel at the western end.

In a fetch-restricted environment such as Point White, waves are generated by locally-occurring winds as no swell source exists. Prevailing wind patterns along the west coast of Canada and the United States are controlled by the locations and intensities of two major semi-permanent atmospheric pressure cells: the Aleutian Low and the North Pacific High (Thomson, 1981). The Aleutian Low increases in intensity as it moves from the Bering Sea to the Gulf of Alaska from August to December and reaches its maximum intensity in January. The North Pacific High remains off the northern Californian

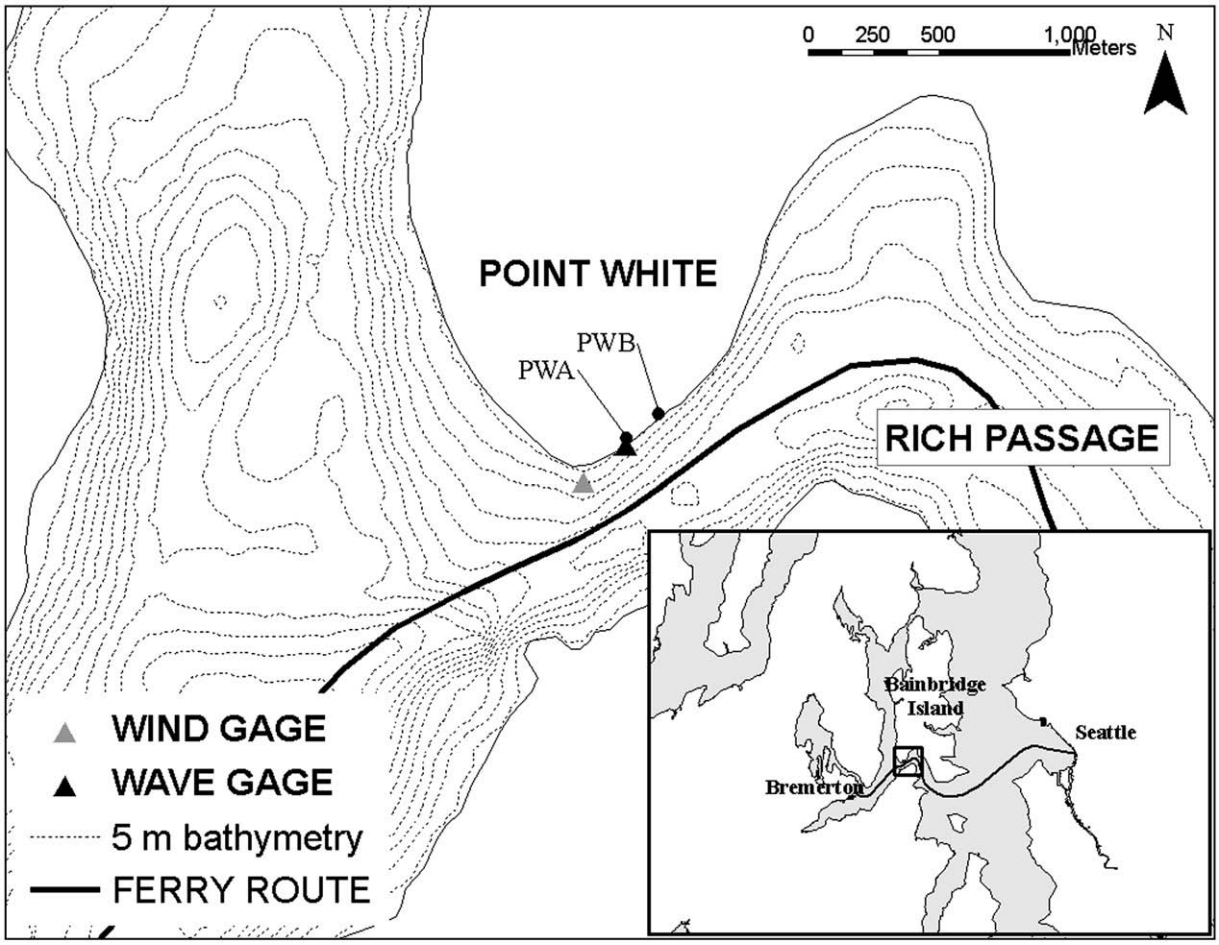

Fig. 1. Study area.

coast year-round but is at a maximum in the summer months. The dominant counter-clockwise rotating Aleutian Low results in predominantly southwest and southeast winds from late fall to early spring along the Northwest coasts. The prevailing winds switch to the northwest from approximately late spring to early fall due to the weakened Low. In Puget Sound, the topography greatly influences the direction and speed of winds. Because of this we collected site specific wind and wave data to develop the wind wave climate. The locations of wind and wave measurements are shown in Fig. 1.

The narrow (~600 m) western end of Rich Passage is exposed to vessel traffic operating in the channel. The primary source of vessel wakes at Point White are Washington State Ferry (WSF) car ferries. WSF operates 26 daily car ferry transits between Seattle and Bremerton. Two vessels of different class primarily operated during the study period: the *MV Walla Walla* (length: 134.1 m, beam: 26.5 m, draft: 4.9 m) and the *MV Kitsap* (length: 100 m, beam: 24.0 m, draft: 5.0 m). The ferries operate at speeds of 13–18 knots through Rich Passage. Other vessels also contribute to the wake climate including recreational boats, commercial fishing vessels, tugboats, US Naval vessels, US Coast Guard vessels, and private charter boats. There is a significant increase in vessel traffic during the recreational boating season from June to September.

3. Materials and methods

3.1. Wind, wave, and current measurements

Site specific data were obtained to characterize the influence of the multiple forcing mechanisms at Point White. Fig. 2 shows a timeline of the data collection at Point White. Wind speed and direction were measured by an anemometer deployed from 26 July 2006 to 8 June 2007 on a USCG Navigational Aid at approximately 12.2 m, mllw. Data were collected at 10 min intervals with a RM Young propeller vane and helicoil integrated with electronics and software. Gaps in wind data were filled using a modeled wind climate assembled from nearby meteorological stations at Seattle-Tacoma International Airport, Bremerton and West Point. The algorithm for creation of the wind record is described in PIEngineering (2007). Wind waves reaching Point White are fetch-limited and aligned with the direction of maximum fetch (9 km from the southwest. Fig. 3 shows a wind rose for winds greater than 5.0 m/s measured at Point White. The dominant wind direction is from the southwest between approximately 200° and 240°, aligned with the axis of the maximum fetch. Fig. 8e shows a time series of wind at Point White. The gray points are wind speeds greater than 5.0 m/s; the black lines are a smoothed maximum and average for wind speeds greater than 5.0 m/s and at least 2 h in duration. Storms with wind speeds larger than 7.5 m/s occurred between late October 2006 and late May 2007. The highest wind speeds recorded occurred during a storm on 13–14 December 2006. This storm is estimated to have a 10-yr return interval based on an extremal analysis of a 31-yr wind record from Seattle-Tacoma International Airport, the longest historical wind record in the vicinity. The maximum wind speed at Point White during the storm was 18.8 m/s.

Wind waves, wakes, and water levels at Point White were measured using a Macrowave pressure-sensing gage deployed from 26 July 2006 to 23 August 2007 at 0.0 m, mllw at PWA. Pressure was recorded at 4 Hz in 34 min bursts. The pressure time series was

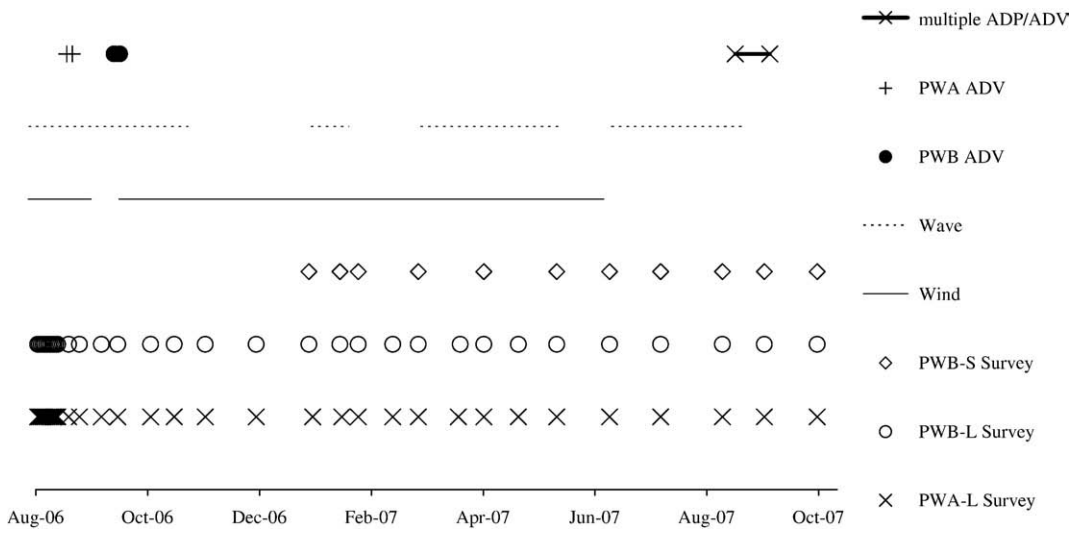

Fig. 2. Timeline for data collection at Point White.

converted to water surface elevation using linear wave theory and the descriptive wave parameters were determined using zero-crossing and spectral analysis. The dominant wind waves originate from the southwest and diffract energy onto beaches in the lee of Point White. Time-averaged descriptive wave parameters including significant wave height, peak period, wind speed and direction measured during four storms at Point White are summarized in Table 1. The time-averaged significant wave height ranges from 0.1 to 0.24 m and the average wave period ranges from 1 to 3 s. The maximum significant wave height was 0.33 m on 7 January 2007. Unfortunately, no wave measurements were recorded during the 10-yr wind storm due to technical difficulties. The water depth for which waves start to mobilize sediment is generally equal to one quarter the wavelength (Soulsby, 1997); thus, observed waves at Point White can begin to disturb sediment as shallow as 0.40 m and at most 3.5 m.

Wind-generated waves at Point White were predicted using a numerical model based on the work of Mase and Kitano (2000), Mase (2001), and Mase et al. (2005). The model is a state-of-the-art, two-dimensional, and spectral, wave transformation model, based on the phase-averaged wave action (energy density) conservation equation. A finite difference method is used to solve the wave action conservation equation. The model capabilities include shoaling,

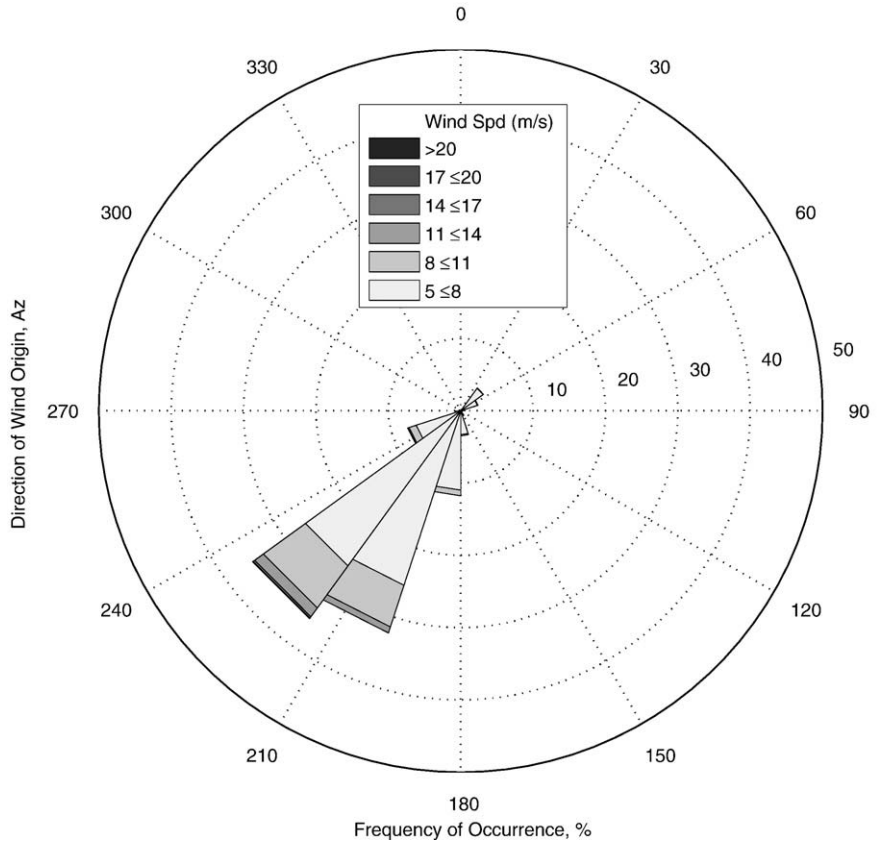

Fig. 3. Directional wind data for winds larger than 5 m/s.

Table 1
Time averaged wind-wave parameters for four storms

Date	Wind speed (m/s)	Wind dir.	Hsig (m)	Tp (s)
7-Jan-07	9.4	210	0.24	2.7
9-Jan-07	7.3	206	0.12	1.1
11-Mar-07	7.1	210	0.11	2.5
9-Apr-07	10.0	217	0.14	2.4

refraction, diffraction, reflection, depth-limited breaking, dissipation, and wave–current and wind–wave interaction. This modeling approach is able to account for the important physical processes that dominate wind–wave growth in Rich Passage (i.e. wind–wave generation, wave–current interaction due to the presence of tidal currents, and diffraction of wave energy from adjacent bodies of water). Validation and application of the model to the study area are described in detail in PIEngineering (2007). The predicted hourly breaking wave height at PWA during the study is shown in Fig. 8f.

The wave record was also used to identify vessel wakes. A one week wave record from 26 July 2006 to 3 August 2006 was analyzed in detail. A WSF operational schedule was used to identify 26 scheduled crossings per day, totaling 182 wakes in a week. The one week wake climate is representative of the yearly wake climate in the absence of wind waves based on an extensive wake climate analysis of Point White during the summer, fall, and winter (PIEngineering, 2007). Non-WSF vessel wakes were identified in the wave record and despite high boat traffic during the summer months they are not considered a significant source of wake energy.

Tidal currents were measured during instrument deployments in August and September 2006 and in August 2007. The instrument setup measured cross-shore variation in currents at PWA and PWB and simultaneously obtained synoptic boat-based measurements of current. 3-D velocity point measurements near the bed were obtained at an offshore (−1.0 m, mllw) and inshore (2.0 m, mllw) location at PWA and PWB from tripod mounted Acoustic Doppler Velocimeters (ADV). Current direction and magnitude in the entire water column were measured using up-looking Acoustic Doppler Profilers (ADP) deployed at −3.5 m, mllw at both PWA and PWB. Synoptic current measurements were obtained from shore normal transects made by a kayak equipped with a miniature ADP. The current measurements provided a characterization of the spatial and temporal patterns of tidal induced velocities in the nearshore along Point White for validation of a two-dimensional circulation model, and to estimate bed shear stress induced by steady currents for estimating sediment mobility.

3.2. Tracer measurements

Direct measurements of pebble and cobble (gravel) transport were obtained at Point White using particle tracking methods. Particle tracking relies on the ability to recover the tracers through time and the assumption that the tracers behave as native sediment (White and Inman, 1989). The first assumption is met by properly preparing tracers to match the size distribution and shape characteristics of the natural sediment. The recovery of tracers through time is made possible using a Radio Frequency Identification (RFID) tracking method, which has proven recovery rates of 80% or more (Osborne, 2005; Allan et al., 2006). The particle tracing technique used is previously described by Allan et al. (2006) and Nichols (2004). The system involves RFID technology, Passive Integrated Transponder (PIT) tags, and Real Time Kinematic — Global Positioning System (RTK GPS) surveying. Tracer particles are fitted with PIT tags and detected by a Radio Frequency/Control module and an antenna. Three different low-frequency PIT tags made by Texas Instruments were used: 32 mm and 23 mm long, tubular-shaped, hermetically sealed (glass encapsulated) transponders and wedge-shaped, polyethylene sealed 12 mm transponders (Fig. 4). The PIT tags require no batteries, as they draw power from an electromagnetic pulse from the reader and antenna unit to transmit their ID number to the detection module.

Fig. 4. RFID transponders — 32, 23, and 12 mm, respectively placed in tracer particles.

Tracer particles are made from samples of surface sediment chosen to match the size and shape of the native distributions as closely as possible but are constrained by the size of the PIT tags. Fig. 5 shows the size distributions of the tracers compared to that of the beach surface particles obtained by pebble counts. The median tracer size is 23 mm. The tracers are underrepresented for sizes between 12 and 25 mm and not represented for sizes less than 12 mm because of the minimum PIT tag size. The tracers are classified by four mean size groups: 16 mm, 22.6 mm, 32 mm, and 45 mm.

Tracers were matched to the shape characteristics of the native beach sediment using sphericity (Sneed and Folk, 1958) and Zingg indices (Zingg, 1935 as cited in Oakey et al., 2005). Both methods use measurements of the long (L), intermediate (I) and short (S) axes of the grain. Sphericity is calculated as: $\sqrt[3]{\frac{S^2}{IL}}$. The Zingg method uses a Cartesian coordinate system to plot four extreme shapes based on the indices S/I and I/L. Each tracer set created has an average sphericity within 2.5% error of the average sphericity of the beach samples. The tracers were graphically compared to the Zingg indices of the beach samples.

Sets of 48 tracers were deployed at PWA and PWB from 1 August 2006 through 5 October 2007 (see Fig. 2 for timeline). The tracers were deployed in a random grid (30 cm spacing) centered at approximately 3.0 m, mllw and surveyed every two to four weeks depending on the tide schedule. The cross-shore location was chosen in order to initiate tracers within the active swash zone on the beach.

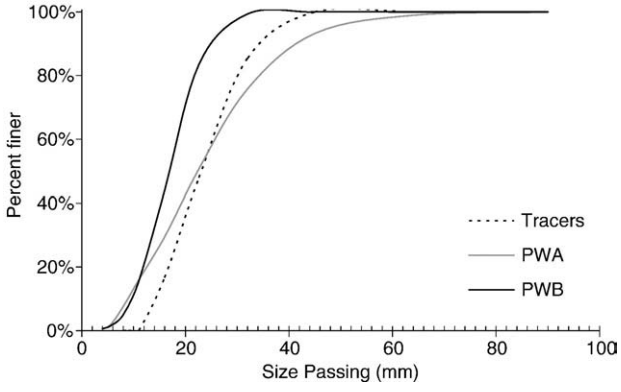

Fig. 5. Size distribution of tracers particles compared to beach surface samples.

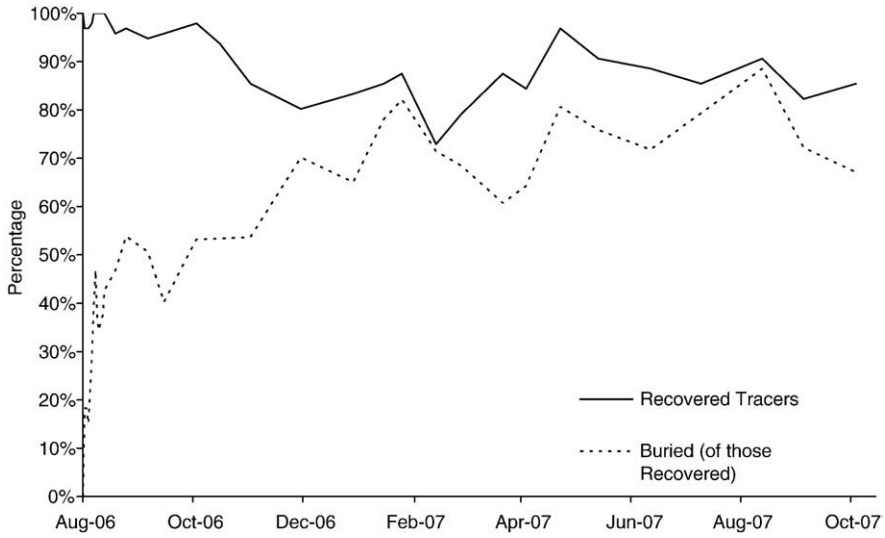

Fig. 6. Percentage of found tracers and buried tracers at sites PWA and PWB combined throughout the study.

A tracer survey consisted of finding the tracers with the RF control module and recording their positions with the RTK-GPS, leaving the tracers undisturbed. Informal testing of the RF control module indicated the largest tracers could be detected up to 40 cm and the smallest tracers could be detected up to 20 cm. The detection capability varied based on the RFID tag orientation in relation to the antenna unit. A shore-normal beach transect of horizontal positions and elevations at each deployment site were also surveyed during each tracer survey. An additional set of tracers was deployed beginning in November 2006 at PWB for sampling and recovery at short intervals and thus denoted as PWB-S. PWB-S was deployed, recovered after four weeks, and then redeployed at the initial site. Occasionally, an intermediate, two week survey was executed to record the tracer locations between deployments.

The RFID tracking methodology provided high recovery rates of the tracers. Fig. 6 shows the percentage of tracers recovered during each survey between August 2006 and October 2007. In general, the recovery is above 80% (min. of 73%) throughout the study. Also shown in Fig. 6 is the percentage of recovered tracers that were not visible on the surface (buried). The percentage of buried tracers increases steadily until early February 2007. Two factors caused the minimum recovery in the winter months: high burial rates because of storms and the difficulty of sampling at low winter tide ranges.

4. Results

4.1. Tracer particles

The particle tracking data were analyzed to determine the magnitude of alongshore and cross-shore transport between survey periods as well as any dominant patterns based on particle size or location on the beach. Fig. 7 is a map of the centroid of the tracers

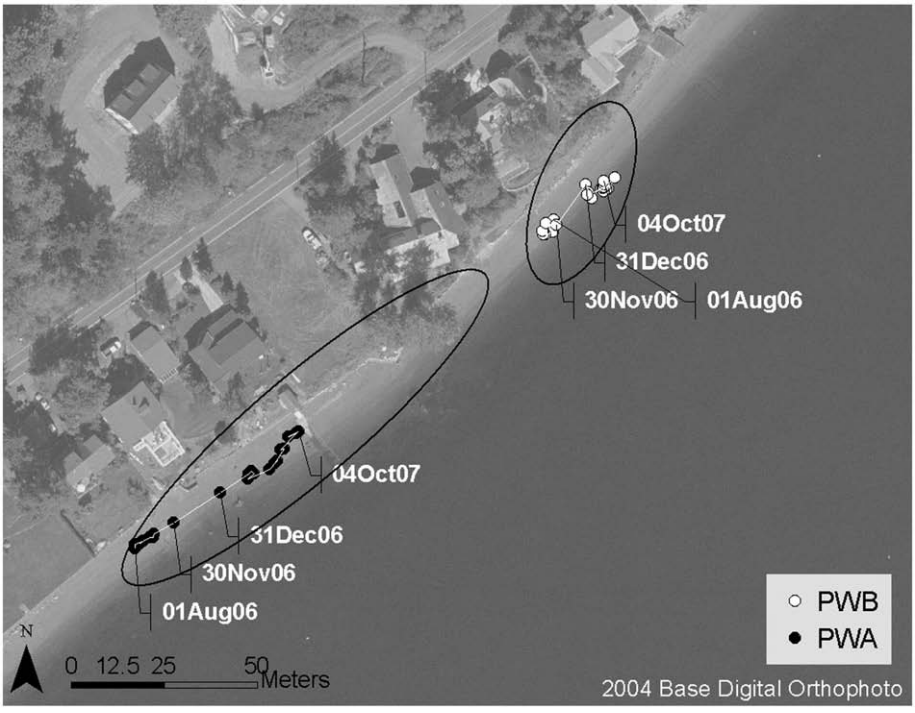

Fig. 7. Spatial map of tracer centroid through time at Point White. Key dates are labeled. The ellipses represent the distribution of the tracers at the final survey in October 2007.

through time. The most noticeable feature is the amplified alongshore movement to the northeast at both sites between November 2006 and the end of December 2006. The alongshore movement is greater at PWA than at PWB.

The centroid distance from the initial deployment position in the alongshore and cross-shore directions at both sites is shown in Fig. 8a, b. Error bars indicate one-half standard deviation from the centroid in the respective direction. The time series of beach slope, wind speed, and breaking wave height are also shown in Fig. 8c–f to compare the wind wave forcing to tracer transport and morphologic response. Tracers at PWA move alongshore at a rate of approximately 0.065 m/day between April and November, while at PWB the rate of movement alongshore is only 0.005 m/day in the same interval. The daily transport rate at PWA increases by a factor of 6 in the period between November and January. At PWB the alongshore transport rate increases by a factor of 90 during the month of December. The transport during December is largely a result of the 10-yr storm that occurred on 13–14 December 2006. The magnitude of alongshore movement in December is similar at both sites. However, the magnitude of alongshore movement during the non-storm intervals is higher at PWA and is possibly explained by site specific differences in wind waves and vessel wakes, which are discussed later. The observed transport in the non-storm interval following the storms may be dampened by the high burial rate of the tracers. The number of tracers that remain buried after the storm interval is an indication that vertical mixing is higher during storms than during the following non-storm interval.

The cross-shore movement of the tracers is a small fraction of alongshore movement. The final cross-shore movement is ~1/18 the final alongshore movement at PWA and a slightly larger fraction, ~1/6, at PWB. Cross-shore movement at both sites fluctuates between onshore and offshore initially but the general trend is offshore during the first week at PWA and the first two weeks at PWB. The tracer movement at both PWA and PWB is slightly offshore from January 2007 to April 2007 and then changes to slightly onshore from April 2007 through October 2007. The cross-shore patterns are more clearly illustrated in Fig. 9, which shows the centroid of four different size classes of tracers by their elevation on the beach through time. Fig. 9 shows there is a trend at PWA for offshore movement of tracers from January 2007 to April 2007 and an onshore movement of tracers from April 2007 to October 2007. The trend is consistent with the observations of cross-shore movement in the tracer centroid. At

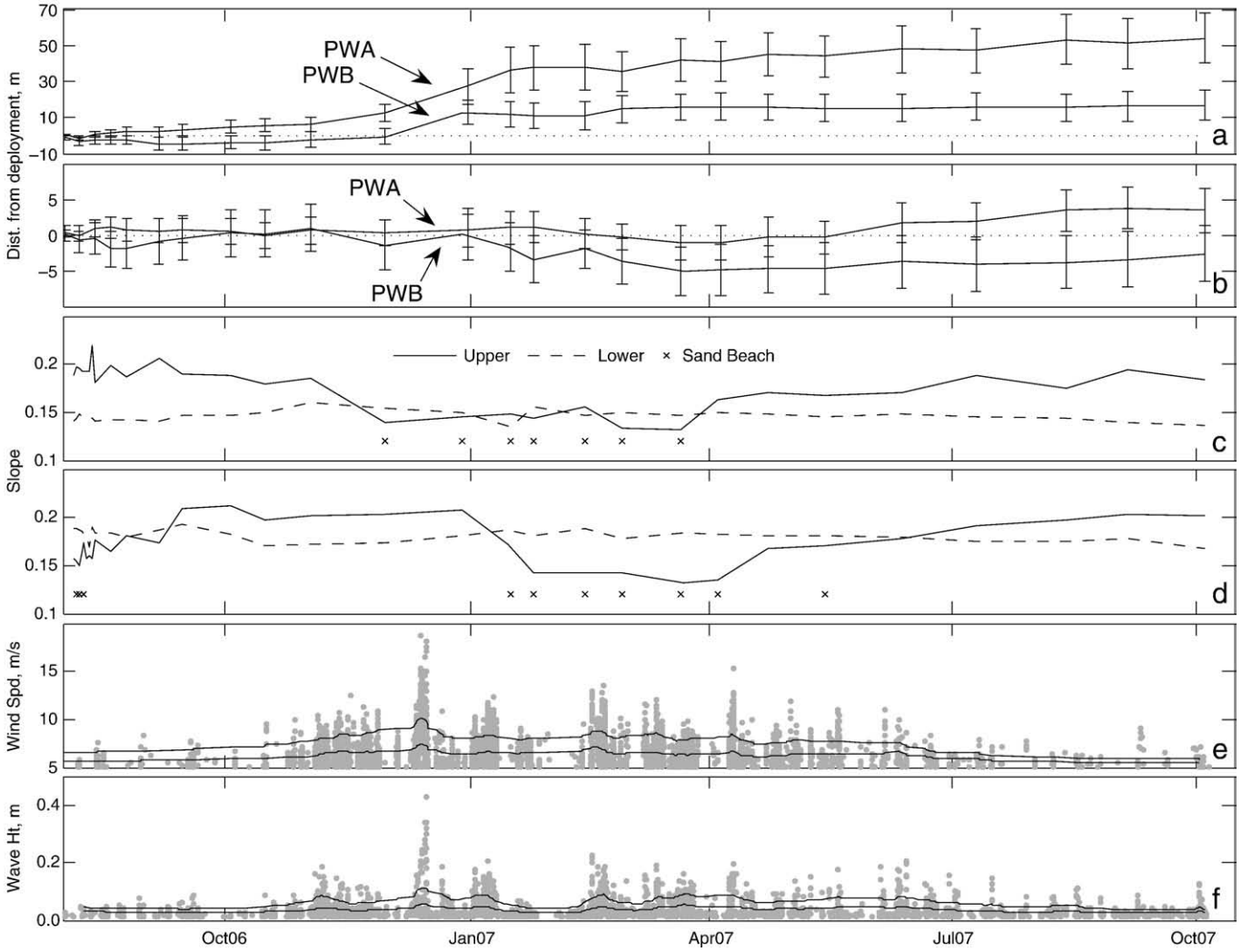

Fig. 8. Net centroid movement from deployment site in alongshore (a) and cross-shore (b) direction. Error bars are +/−1/2 standard deviation from the centroid. Positive is onshore and alongshore to the NE. Negative is offshore and alongshore to the SW. Slope of upper and lower beach at PWA (c) and PWB (d). 'x' indicates sandy upper beach. The slope varies between 0.13 and 0.22 on the upper beach and 0.13 and 0.19 on the lower beach. (e) Time series of wind speed at Point White. Gray points are all measured wind speeds over 5 m/s. The upper black line is a smoothed maximum wind speed for storms at least 2 h in duration. The lower black line is a smoothed average wind speed for storms at least 2 h in duration. (f) Time series of predicted hourly breaking wave height at PWA. The upper black line is a smoothed maximum wind speed for storms at least 2 h in duration. The lower black line is a smoothed average wind speed for storms at least 2 h in duration.

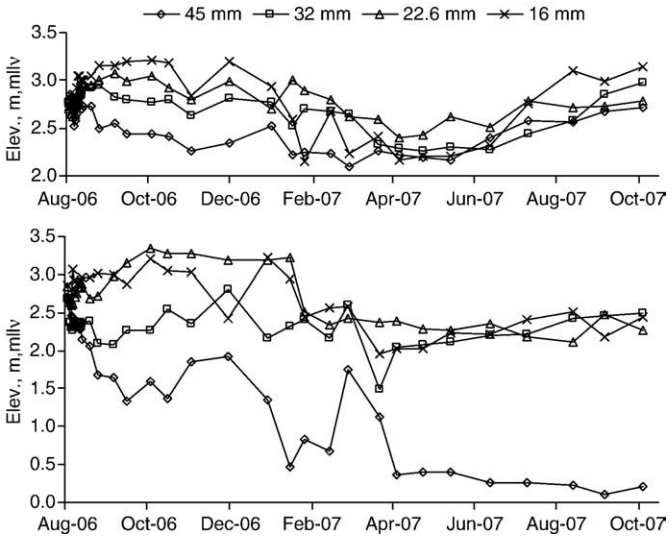

Fig. 9. Elevation of tracers grouped into four size classes at PWA (upper) and PWB (lower). Tracers are well sorted according to elevation and size within two weeks of the initial deployment.

PWB there is a trend for offshore movement of the tracers from February 2007 to April 2007 and a gradual return onshore of the smallest tracers in the following months.

The distribution of different sized tracer particles on the beach varies during the study, between a well-mixed state where all particle sizes are observed equally on the upper and lower beach, and a well-sorted state, where larger (smaller) particles tend to accumulate on the lower (upper) beach. Two events are observed that causes the particles to become sorted (Fig. 9). First, initial sorting at both sites occurred within one to two weeks of deployment. The largest size particles, 45 mm, at mid-beach at PWB were larger than the sediment distribution at the deployment location and were quickly transported to lower elevations. Second, the tracers at both sites become well-mixed across the beach from January 2007 to April 2007 during the storm interval. The tracers at PWA re-sort in the following non-storm interval. PWB remains unsorted with the exception of the largest tracers which remain on the lower beach. Nordstrom and Jackson (1993) also observed the trend for gravel sorting to become homogenous (well-mixed) across the beach during high-energy intervals and heterogeneous (well-sorted) across the beach during low-energy intervals. Grain size appeared to be a much better predictor of behavior than grain shape; no clear trend in transport was found related to grain shape or sphericity.

Alongshore patterns were also observed in the tracer particles. The tracers highest on the beach were transported farther than tracers lower on the beach. The shape of the resulting distribution of tracers is elliptical (Fig. 7), with the longest axis in the direction of alongshore movement. At PWB, 10–15 of the tracers moved alongshore in a gravel berm in the upper foreshore where the beach and revetment meet. Larger and more immobile tracers are located lower on the beach.

Short term tracers were introduced at PWB to determine if the high percentage of buried tracers might be masking short term transport trends. Tracers, PWB-S were deployed and recovered on one month intervals from November 2006 through October 2007. Fig. 10 shows a comparison of daily alongshore transport rate for each survey period for the long term tracers, PWB-L, and the short term tracers, PWB-S, where positive is towards the northeast and negative is towards the southwest. The comparison reveals a trend in transport to the southwest from May to September in the short term tracers that is not recorded in the long term tracers at PWB. The reversal of transport in the alongshore direction implies a change in the relative influence of forcing mechanisms at the site which will be discussed later. The difference in results between the long term tracers and short term tracers also serves as a cautionary note for future studies. The actual transport magnitude may be overestimated for short term tracer deployments because of the rapid sorting that occurs in the first two weeks after deployment; however, the one-month transport estimates are anticipated to be representative of sediment transport trends based on the sorting patterns observed in both short term and long term tracers. Our results suggest that a minimum deployment time of one to two weeks is necessary for accurate representation of transport processes. We also anticipate that this threshold may be different in environments with different forcing levels.

4.2. Morphologic response

Fig. 8c and d is a time series of beach slope at PWA and PWB, respectively, determined from beach profile survey measurements between August 2006 and October 2007. Two estimates for slope are provided: one for the upper profile above 2.5 m, mllw and one for the lower profile below 2.5 m, mllw. The observations of a transition from a steep upper beach to a flat upper beach are temporally consistent with the offshore movement of tracers in Fig. 9 and highlight a temporal lag in the morphologic response between PWA and PWB. The storm condition results in an upper beach slope of approximately 0.14 and the non-storm condition results in an upper beach slope between 0.18 and 0.22. The upper beach is primarily composed of an unconsolidated gravel layer but sand is observed on the upper beach when it is flattened during storm conditions. The overall beach slope at PWB is on average 0.18, higher than at PWA where the average slope is 0.15. Volumetric changes to the upper, lower, and overall beach profile are on the order of 0.75 m^3/m of beach or less. The total volume remains relatively constant across the entire profile throughout the year. In general, the volumetric changes are small, which is consistent with observations by Finlayson (2006) that volumetric changes to beach profiles in Puget Sound are minimal on seasonal scales.

4.3. Nearshore currents

The nearshore currents are highly asymmetric at Point White. Fig. 11 shows a time series of water depth, depth-averaged current speed and direction during a spring tidal cycle acquired using our up-looking ADP deployed at −3.5 m, mllw near PWB. Depth-averaged currents during the flood are aligned parallel to shore and the maximum current speeds average 1.1 m/s. Ebb currents briefly align

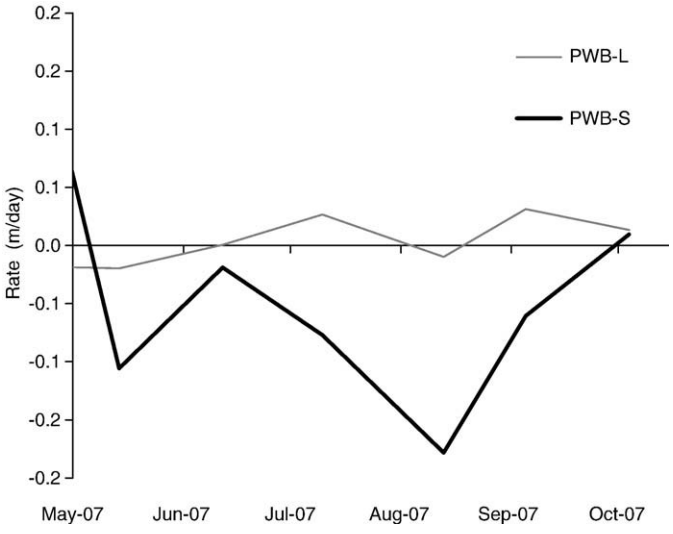

Fig. 10. Comparison of short term and unburied long term tracer transport. Positive is alongshore to the northeast, negative is alongshore to the southwest.

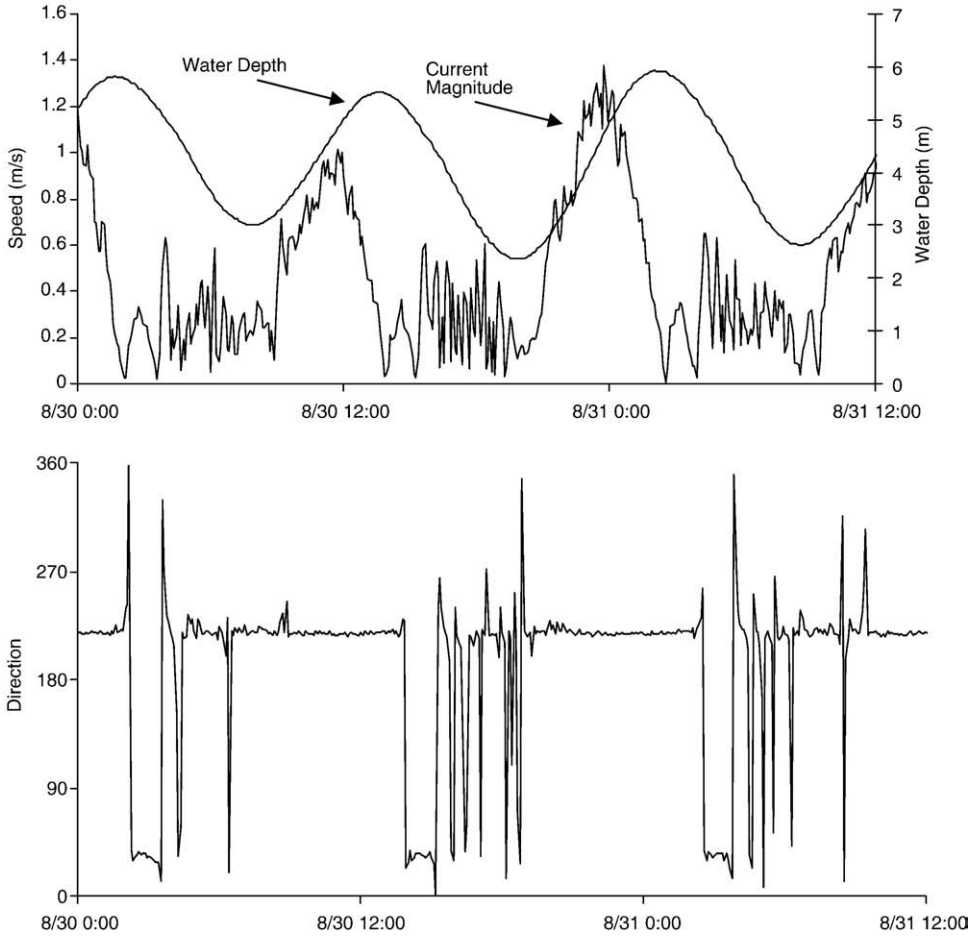

Fig. 11. Measured time series of water depth (upper), depth-averaged current speed (upper) and direction (lower) during a spring tidal cycle acquired using an up-looking ADP deployed at −3.5 m, mllw near PWB. Depth-averaged currents during the flood are aligned parallel to shore at 224° and the maximum current speeds average 1.1 m/s. Currents during the ebb are briefly aligned parallel to shore at 33° for 2 h then become highly variable in direction and speed. The average ebb current is 0.4 m/s.

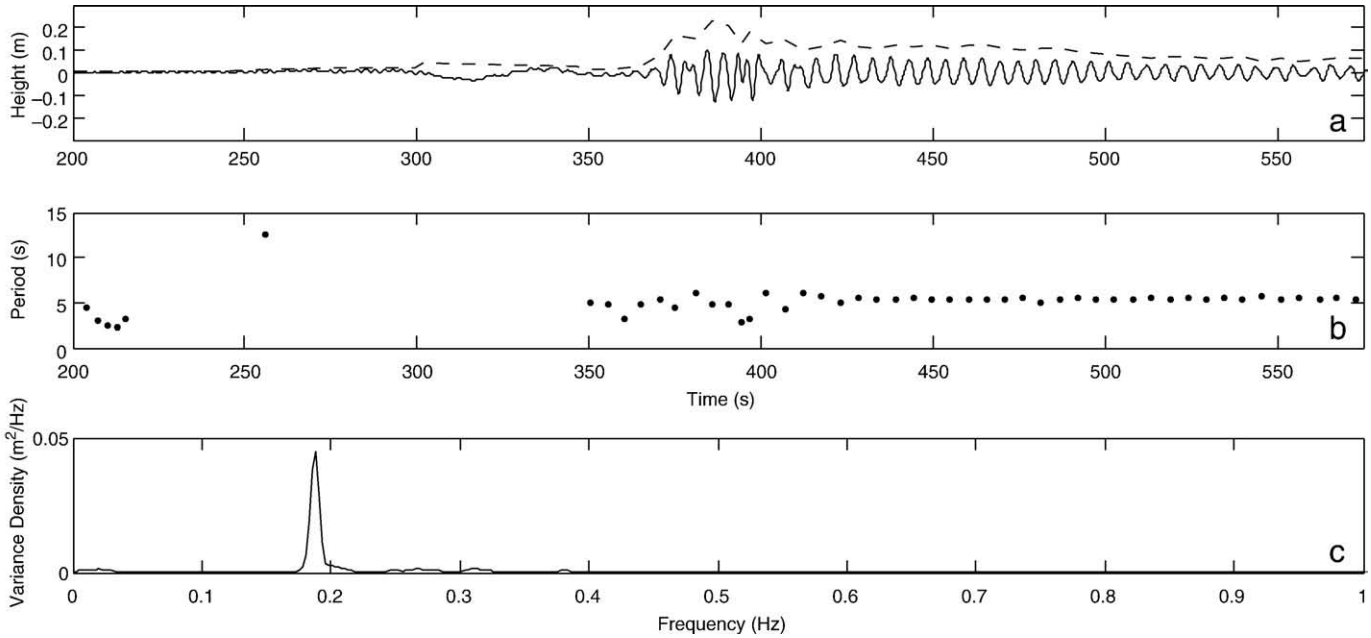

Fig. 12. Wake record for a Seattle bound WSF car ferry. (a) Dashed line is wave height determined from an upcrossing analysis, solid line is water surface elevation. (b) Wave period. (c) Spectral density. Note: time on the *x*-axis is referenced to the start of the instrument data collection burst.

parallel to shore then become highly variable in both speed and direction for the remainder of the ebb tide due to the presence of a recirculation eddy that forms in the bay east of Point White. Depth-averaged ebb currents average 0.4 m/s. The boat-based velocity transect measurements confirm the formation of a nearshore recirculation eddy shortly after ebb tide begins. Peak near-bed velocities measured by ADVs were 0.75 m/s and 0.4 m/s at −1.0 m, mllw and 2.0 m, mllw, respectively. Nearshore currents at PWA are similar in direction and slightly stronger in magnitude than at PWB.

4.4. Vessel wakes

There is a large variance in the observed WSF car ferry wakes at Point White because of sensitivity to the vessel length, draft, and dynamics (speed and track) and water elevation (tide). Fig. 12 shows a time series analysis of water surface elevations measured during a wake from a Seattle-bound car ferry. The car ferries are displacement vessels that produce a typical sub-critical wake in Rich Passage. The water surface elevation (Fig. 12a) is typical sub-critical wake. A sub-critical wake is composed of a diverging bow wake and a transverse stern wake, which travels perpendicular to the sailing line. A maximum wave height (dashed line) is observed in the leading group of waves composed of both a diverging and transverse wake. The divergent wake dissipates quickly and the majority of the wake is composed of the transverse wake, which persists here for nearly 3 min with a steadily decaying wave height and constant period (Fig. 12b). The majority of the wake energy is contained at a single frequency with a peak at 0.19 Hz (Fig. 14c).

The results of the analysis of one week of wake records (182 total wakes) are presented below. The wake spectra of the car ferries are generally monochromatic; peak periods range between 3 s and 6 s (e.g. Fig. 12c). The average of the maximum wave height associated with a wake is 0.23 m (Table 2), but the standard deviation is 0.10 m, indicating there is a large variance in the wakes recorded at Point White. There is only a small difference in the average for the two directions of ferry transit. Another parameter used to describe wakes and reported in Table 2 is the energy flux (a function of the wave height and period) of a wake train. Approximately 63% of the energy flux during the time interval analyzed originates from ferry wakes. The average energy flux per wake train is 8600 J/m of wave crest width and the standard deviation is 8100 J/m. However, the average energy flux in a wake propagated from a ferry traveling from Bremerton to Seattle is nearly twice (10,100 J/m versus 6600 J/m) that of a ferry traveling from Seattle to Bremerton. This is a result of the orientation of the vessel sailing line relative to the shoreline; the ferry leaving Bremerton approaches Rich Passage sub-parallel to the shore resulting in increased exposure of the shoreline to the transverse portion of the wake. A vessel traveling from Seattle is required to turn southwest just prior to passing Point White, resulting in a smaller exposure of the transverse wake to the Point White shoreline. A visual inspection of the wake records confirmed this idea. A clear transverse wake was present approximately 5 times more often in the time series of a ferry traveling from Bremerton compared with a ferry traveling from Seattle.

Table 2
WSF ferry wakes descriptive parameters

Energy (J/m)			Maximum wave height in a wake train (m)		
All wakes	Seattle to Bremerton	Bremerton to Seattle	All wakes	Seattle to Bremerton	Bremerton to Seattle
8600 (8100)	6600 (5900)	10,100 (9100)	0.23 (0.10)	0.24 (0.12)	0.22 (0.09)

One week average (standard deviation).

Table 3
Comparison of predicted bed shear-stresses for combinations of forcing mechanisms at Point White

	H^a (m)	T^a (s)	h (m)	$\overline{\mu}$ (m/s)	τ_b (N·m^{-2})	τ_b/τ_c
(a) In 2 m of water at mean tide level (2 m, mllw)(2m, mllw)						
Peak wind wave	0.33	2.4	2	–	3.8	0.21
Ferry wake	0.23	5.0	2	–	3.2	0.18
Flood current	–	–	2	1.01	5.7	0.32
Current and peak wind wave	0.33	2.4	2	1.01	9.4	0.53
Current and ferry wake	0.23	5	2	1.01	9.0	0.51
(b) At wave breaking on upper beach (~3.5 m, mllw)						
Peak wind wave	0.34	2.4	0.43	–	25.3	1.42
Ferry wake	0.35	5.0	0.45	–	20.6	1.16
Flood current	–	–	0.45	65.1	3.6	0.20
Current and peak wind wave	0.34	2.4	0.43	64.0	27.8	1.56
Current and ferry wake	0.35	5.0	0.45	65.1	23.1	1.30

[a] H_s and T_s for wind waves, H_m and $T@H_m$ for ferry wakes.
Bed shear-stresses are calculated based on a median grain size of 20 mm. Critical shear stress for a 20 mm size grain is 17.8 N·m^{-2}. Calculations are shown for two cross-shore locations on the beach at the same tidal phase: (a) mean tide level at 2 m of water depth, and (b) on the upper beach at wave breaking depth.

4.5. Comparison of forcing mechanisms

The potential for gravel entrainment and transport on the beach is quantified by a comparison of the predicted bed shear-stress, τ_b, induced by the forcing mechanisms relative to the predicted critical bed shear-stress, τ_c, required to mobilize a sediment grain. Estimates of τ_b, τ_c, and the ratio τ_b/τ_c, are shown in relation to water depth, h, depth-averaged current velocity, $\overline{\mu}$, the significant wave height and period, H_s and T_s, for wind waves, and characteristic maximum wave height and corresponding wave period, H_m and $T@H_m$, for ferry wakes in Table 3. Bed-shear stresses are shown for a combination of wind waves, ferry wake waves, and currents during a flood tide at two cross-shore locations on the beach: 2 m water depth and at wave breaking depth. The τ_c for a 20 mm median grain size (D_{50}) is 17.8 N·m^{-2} for a single-sized sediment bed (Soulsby and Whitehouse, 1997 as cited in Soulsby, 1997) and bed shear-stresses are calculated based on the methods of Soulsby (1997). The ratio τ_b/τ_c is shown in order to compare the potential for transport under the various forcing mechanisms. The results show that τ_b is typically less than $0.5\tau_c$ for all forcing mechanisms at 2 m water depth. However, it is shown that τ_c is exceeded at wave breaking for peak wind waves ($\tau_b/\tau_c = 1.42$), ferry wake waves ($\tau_b/\tau_c = 1.16$), and both in combination with flood currents ($\tau_b/\tau_c = 1.56$ and 1.30). The ratio τ_b/τ_c for tidal currents is 0.32 and 0.20 at 2 m and 0.45 m water depth, respectively. τ_b under the peak wind waves at breaking increases by approximately 10% in the presence of a tidal current. This implies that tidal currents alone are not strong enough to mobilize gravel-sized sediment but they may enhance stresses at wave breaking, in addition to affecting the directionality of alongshore transport. These estimates of relative shear stress are provided only as an illustration of the relative contributions of the forcing mechanisms to gravel transport. However, caution should be exercised in their application because they are based on the assumption of a sediment bed composed of a single grain size rather than a mixed-sediment bed.

5. Discussion

The tracer observations, profile measurements, and hydrodynamic measurements indicate that processes on the Point White beach exhibit two different modes of behavior during the storm and non-storm intervals. During the storm interval from November to April

gravel transport at Point White is dominated by wind waves that move gravel primarily alongshore toward the northeast. Fig. 13 shows a temporal comparison between the alongshore gravel transport observed in each survey period and the maximum wind speed for the same period. A linear regression analysis of wind speed and transport yields R^2 values of 0.72 and 0.73 for PWA and PWB, respectively, during the storm interval, and 0.29 and 0.25 during the non-storm interval. Thus, wind waves and alongshore transport are strongly correlated during the storm interval, but not during the non-storm interval.

During the non-storm interval from May to October, alongshore transport is small compared to transport during the storm interval. The lack of correlation between wind and alongshore transport in the non-storm interval indicates that other forcing mechanisms such as ferry wakes and tidal currents likely contribute to the sediment transport during the non-storm interval. The reasons for the difference in the direction of alongshore transport between the two sites during the non-storm interval is unclear. At PWB the alongshore movement of the long term tracers was almost non-existent in the non-storm interval following the storms, however, the short term tracers recorded a slight net transport to the southwest. The predicted bed shear-stresses suggest that a combined ferry wake and flood current are a possible mechanism for gravel transport. The layer of gravel mobilized by combined ferry wakes and tidal currents appears to be thinner than that mobilized by wind waves as evidenced by the minimal transport of buried long term tracers at PWB following the storm interval. At PWA, the tracers continue to move to the northeast in the non-storm interval. One reason for the transport to the northeast could be the increased exposure to the higher energy, transverse ferry wake waves propagating from a Seattle-bound ferry. Another hypothesis for the northeast transport at PWA is that the site is more exposed to the few wind waves that occur during the non-storm interval; however, the maximum wind speed and the transport are not well-correlated during this period (Fig. 13).

The observations indicate that both cross-shore and alongshore processes contribute to the seasonal morphologic response of the beach. Fig. 8 shows the temporal correspondence between transport, morphology, and forcing conditions. Observations confirm that morphologic response varies alongshore at Point White. The temporal and spatial patterns of alongshore transport are consistent with observations that gravel moves alongshore in stages (RPWAST, 2001). The morphologic fluctuation in upper beach slope and sediment size composition at PWA corresponds to the largest alongshore transport of the tracers but the morphologic fluctuation at PWB is time-lagged. It is interesting that the identical morphologic patterns are observed at both sites but occur at different times during the year. The exact reason for the time-lag is unclear but one hypothesis is that it is related to the thicker layer of gravel at PWB (down-drift of PWA) delaying the appearance of a flatter, sandy beach. In the cross-shore direction there is a temporal consistency between patterns of cross-shore elevation of tracers (Fig. 9) with the fluctuations in the beach profile (Fig. 8c, d). However, the comparison of the cross-shore transport of the tracers (Fig. 8b) to the fluctuations in beach profile (Fig. 8c, d) does not show a clear correspondence except that there is generally an onshore trend of gravel during the non-storm interval when the upper beach slope also increases. The exact timing and importance of alongshore and cross-shore transport to the observed morphologic fluctuations appears to be quite complicated and not fully resolved by our measurements. The interpretation of the observations may be hindered by the burial of tracers and the spatial variation of the tracers in relation to the beach survey transects. The alongshore variability in morphology also makes it difficult to interpret the overall response based on only two transects.

The morphologic fluctuations generally correspond to the seasonal change in wave energy. The flattening of the upper beach corresponds to increased storm wave forcing. This is consistent with the findings of Quick and Dyksterhuis (1994), Kirk (1975), and Dawe (2006), who find that high wave attack on MSG beaches causes offshore transport of gravel and beach flattening. The morphologic response is also consistent with the model for low-energy beaches provided by Nordstrom and Jackson (1993) in which high energy waves erode sediment on the upper beach and low energy waves accrete sediment on the upper beach. In contrast to these previous findings on MSG beaches, cross-shore transport at this site is not the only process driving morphologic response. Alongshore transport appears to make a significant contribution to the morphologic response. The relative steepness of the beach at Point White limits the modification of oblique waves as they approach shore and results in a substantial portion of alongshore transport in comparison to transport on a milder sloping beach.

A shift to a stable, coarse sand composition on the upper beach is a distinct characteristic of the storm condition on the beach. The observations are consistent with a reverse winnowing process, in which the gravel is more mobile than the fine fraction. However, we

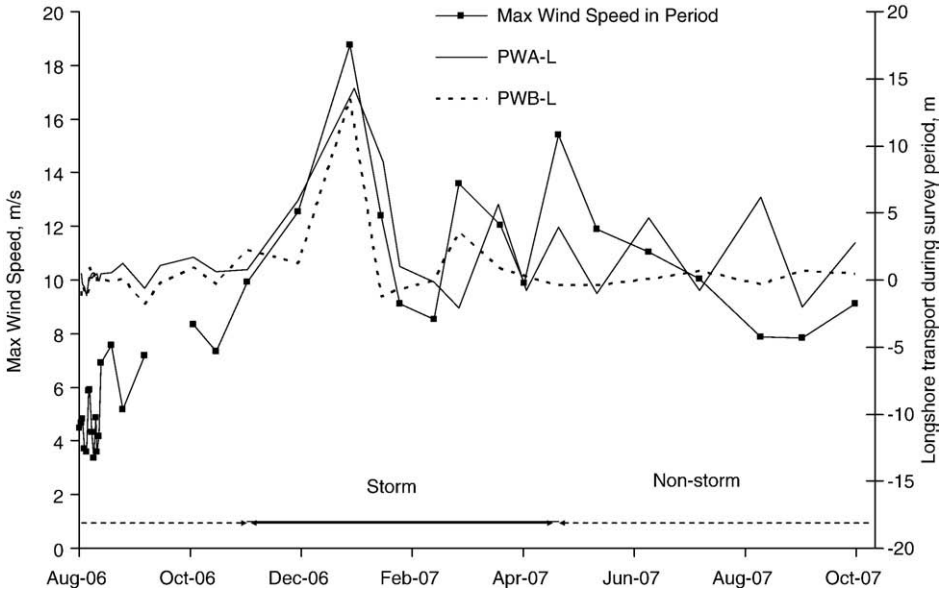

Fig. 13. Max wind recorded at Point White NAVAID correlated with alongshore tracer movement per survey period at PWA and PWB.

cannot be certain of the sand behavior without direct measurements of the fine fraction. After the cessation of storm waves, gravel slowly accretes on the upper beach. Ferry wakes appear to be a mechanism for post-storm recovery of gravel on the upper beach. Tidal currents are not a likely mechanism because they are not strong enough to mobilize gravel-sized sediment. Such changes in beach composition, which may be somewhat unique to MSG beaches, are very challenging to model and difficult to observe due to their spatial heterogeneity and the long timescales over which they occur. Although the dynamical details related to this observed shift in beach composition are not well-resolved in the current study, it is a striking feature of the seasonal variability on the beach and, thus, likely to be important in the overall morphological and sediment transport regime.

The seasonal behavior of gravel erosion on the upper beach during storms and gravel accretion during calm intervals is opposite the behavior of cobble berms on sand and cobble beaches observed by Everts et al. (2002) on the southern California coast. The cobble berm dynamics are explained by the seasonal differences in wave height and internal berm properties. Large waves and a small sand to cobble ratio in the winter increase onshore swash intensity and cause accretion of cobble to the berm. Small waves and a large sand to cobble ratio in the summer increase backwash intensity and cause erosion of the cobble berm. At Point White it is not clear how the interrelationship of wave energy, grain size composition, and beach slope, alter the swash velocities. Sustained high energy waves and the low permeability of the upper beach may result in increased backwash that erodes gravel from the upper beach until a stable sand beach slope is reached. A subsequent reduction in wave energy results in swash velocities that promote gravel accretion on the upper beach.

The relative contributions of the forcing mechanisms at Point White are summarized as follows: Tidal currents cannot mobilize sediment but can enhance sediment transport in the direction of the flood tide. Car ferry wakes, which typically provide sufficient bottom stresses to mobilize sediment, contribute to sediment transport and the seasonal fluctuations in morphology. The combination of wakes and tidal currents provide a mechanism for alongshore and cross-shore transport. However, the direction of alongshore transport is not clear under ferry wakes and is site specific due to the variability in wake propagation paths. Ferry wakes also appear to provide post-storm recovery, redistributing sediment onshore. Wind waves are the dominant mechanism for alongshore sediment transport, the magnitude is controlled by the site specific wind wave exposure. Wind waves also move gravel offshore and are a key contributor to the morphologic response cycle.

Although the period of our study was unique in its duration, considerable variability also occurs at longer time scales that likely have an important influence on transport at this site. The morphologic measurements showed a fluctuation in the beach profile sediment volumes and a return to the original sediment volume at the end of the measurement interval. The cyclic offshore/onshore pattern of tracers is consistent with the morphologic response, but this does not occur in the alongshore direction. The imbalance of sediment in the alongshore direction should cause the beach to gradually erode because the system appears to be supply-limited to the southwest and landward. Three hypothetical scenarios may explain this: (1) The beaches are erosive on a longer scale than the measurement interval. (2) The sediment transport observation period is not long enough to witness a full cycle of sediment exchange alongshore. (3) The tracers over-emphasize alongshore transport in the gravel berms and the small reversal of alongshore transport is enough to replenish sediment to the upper profile.

All three hypotheses may help explain the imbalance of transport observed in the tracer experiment. Fig. 14 shows a timeline of ferry operations in Rich Passage and the volumetric change to the upper and lower profile (above and below mean tide level) from the last seven years at PWB relative to May 2000. The introduction of high speed ferries in 2000 initially resulted in erosion from the upper foreshore and accretion on the lower foreshore. The lower foreshore eventually eroded as well. Between 2004 and the time of this study the entire beach was slowly accreting sediment. The profile does not indicate beach erosion over the past seven years but the profile changes could be complicated by the residual effects of post-fast ferry recovery. It is also difficult to conclude the beach is erosive on this time scale based on anecdotal beach observations from property owners that the sediment volumes have not changed in the past few decades (with the exception of the erosion caused by the high speed ferry wakes) despite the seasonal fluctuations of sediment. It is plausible, though, that the beach is erosive on a much longer time scale due to the limited supply of sediment. The observational period may not be long enough because of the high burial rates of the tracers near the end of the experiment. The buried tracers may not be uncovered and return towards the deployment location for several years. This highlights the need for long term observations to make accurate predictions of transport on low-energy beaches. Also, caution should be exercised in interpreting sediment transport from the gravel tracers. The measurements are useful for determining the patterns of transport but may not accurately reflect the transport of the whole range of beach sediment. The measurements could be improved by

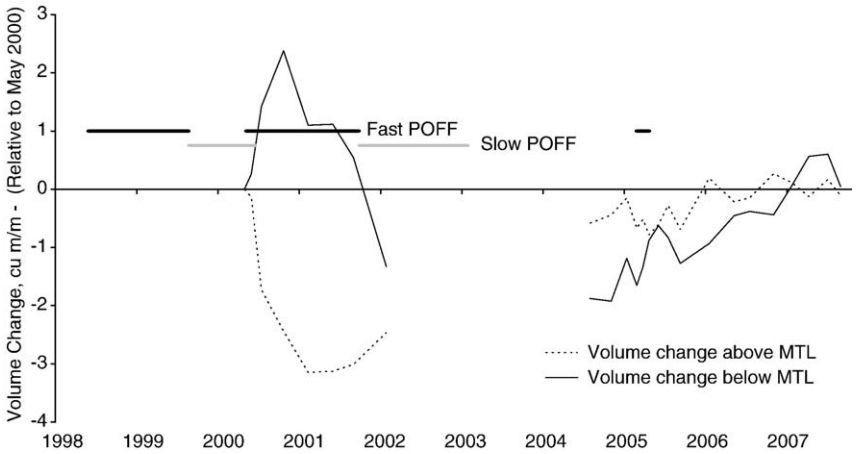

Fig. 14. Volume change at PWB over an 8 yr time period relative to May 2000 above (dashed line) and below (solid line) mean tide level. The timeline of operation of the passenger only fast ferry (POFF) operating at fast and slow speeds is also shown. The long term data indicate the beach is not erosive, however the data set is complicated by the residual effects of post-fast ferry recovery.

using tracers that more closely represent the grain size distribution of the beach. The tracers used underrepresented 60% of the surface grain size distribution of the beach. Additionally the methods could be improved by continually adding more tracers to the system and leaving them on the beach rather than short term sampling of the tracers as performed at PWB. Comparisons between the short term tracers and long term tracers are made difficult because of the initial cross-shore sorting of the sediment.

6. Conclusions

Direct measurements of coarse sediment transport on a mixed sand and gravel beach at Point White reveal the transport to be dominated by wind waves in a primarily uni-directional process alongshore towards the northeast. Storminess and site specific exposure to wind waves controls the magnitude of alongshore transport, which occurs primarily from November to April. During the non-storm interval ferry wakes and tidal currents are the primary contributions to cross-shore and alongshore transport. The morphologic response of the beach is evident in a seasonal fluctuation of the upper beach profile in slope from steep to flat and in sediment composition from gravel to coarse sand. Our findings highlight the need to incorporate changes in beach composition into modeling of MSG beaches to accurately predict the response, as well as the need for accurate wake wave propagation modeling to predict site specific response to wakes. The field measurements of transport and morphology support the previous ideas concerning MSG beach response and provide an unusually long data set that can be used to verify model predictions. However, they also highlight a number of seasonal patterns that occur on MSG beaches that cannot be observed in shorter time-scale studies.

Acknowledgements

This study is funded under a federal grant program administered by the Federal Transportation Administration (FTA-WA-26-7007-2005), designed to support research and investigations of emerging transportation systems. This work would not have been possible without the cooperation and assistance of many people: past and present PI Engineering staff have assisted with data collection and processing; the waterfront property owners of Rich Passage have provided access to beaches, and the vessel operators have provided the wakes and vessel performance information. Their contributions are gratefully acknowledged.

References

Abbe, T., Goodwin, P., Williams, P., 1991. Marsh erosion by wave action. Coastal Zone, vol. 91. American Society of Civil Engineers, New York, pp. 1747–1761.

Allan, J.C., Hart, R., Tranquili, V., 2006. The Use of Passive Integrated Transponder (PIT) Tags to Trace Cobble Transport in a Mixed Sand-and-Gravel Beach on the High-Energy Oregon Coast, USA.

Burke, A.E., 2003. Observations of gravel sediment transport under vessel generated waves in the Marlborough Sounds. University of Auckland, New Zealand. Master of Science thesis.

Buscombe, D., Masselink, G., 2006. Concepts in gravel beach dynamics. Earth Science Reviews 79, 33–52.

Dawe, I. 2006. Longshore transport on a mixed sand and gravel lakeshore. University of Canterbury, New Zealand. PhD dissertation.

Everts, C.H., Eldon, C.D., Moore, J., 2002. Performance of cobble berms in southern California. Shore and Beach 70 (4), 5–14.

Finlayson, D., 2006. The Geomorphology of Puget Sound Beaches. Puget Sound Nearshore Partnership. Technical Report.

Haugerud, R.A., 2005. Preliminary Geologic Map of Bainbridge Island, Washington. Open-File Report 2005-1387. Department of the Interior. USGS. http://pubs.usgs.gov/of/2005/1387/.

Isla, F.I., 1993. Overpassing and armouring phenomena on gravel beaches. Marine Geology 110, 369–376.

Ivamy, M.C., Kench, P.S., 2006. Hydrodynamics and morphological adjustment of a mixed sand and gravel beach, Torere, Bay of Plenty, New Zealand. Marine Geology 228, 137–152.

Jennings, R., Shulmeister, J., 2002. A field based classification scheme for gravel beaches. Marine Geology 186, 211–228.

Kirk, R.M., 1975. Aspects of surf and runup processes on mixed sand and gravel beaches. Geografiska Annaler. Series A. Physical Geography 57, 117–133.

Kirk, R.M., 1980. Mixed sand and gravel beaches: morphology, processes and sediments. Progress in Physical Geography 4 (2), 189–210.

Kirkegaard, J., Kofoed-Hansen, H., Elfrink, B., 1998. Wake wash of high speed craft in coastal areas. Proceedings of the 26th International Coastal Engineering Conference, Copenhagen, Denmark, pp. 325–337.

Kuehnle, R.A., 1993. Incipient motion of sand–gravel sediment mixtures. Journal of Hydraulic Engineering 119, 1400–1415.

Kulkarni, D.C., Levoy, F., Monfort, O., Miles, J.R., 2004. Morphological variations of a mixed sediment beachface (Teignmouth, UK). Continental Shelf Research 24, 1203–1218.

Lopez de San Roman-Blanco, B., Holmes, P., 2002. Further insight on behaviour of mixed sand and gravel beaches — large scale experiments on profile development. Coastal Engineering 2651–2663.

Mase, H., 2001. Multi-directional random wave transformation model based on energy balance equation. Coastal Engineering Journal 43 (4), 317–337.

Mase, H., Kitano, T., 2000. Spectrum-based prediction model for random wave transformation over arbitrary bottom topography. Coastal Engineering Journal 42 (1), 111–151.

Mase, H., Oki, K., Hedges, T., Li, H.J., 2005. Extended energy-balance-equation wave model for multi-directional random wave transformation. Ocean Engineering 32, 961–985.

Mason, T., Voulgaris, G., Simmonds, D.J., Collis, M.B., 1997. Hydrodynamics and sediment transport on composite (mixed sand/shingle) beaches: a comparison. Coastal Dynamics 97, 48–57 ASCE.

Mason, T., Coates, T.T., 2001. Sediment transport processes on mixed beaches: a review for shoreline management. Journal of Coastal Research 17 (3), 645–657.

McDonald, S., 2003. Wake wash characteristics within confined coastal waters. University of Auckland, New Zealand. Master of Science thesis.

Nichols, M.H., 2004. A radio frequency identification system for monitoring coarse sediment particle displacement. Applied Engineering. Agriculture, 2004. 0883-8542, Vol. 20(6). American Society of Agricultural Engineers, pp. 783–787.

Nordstrom, K.F., Jackson, N.L., 1993. Distribution of surface pebbles with changes in wave energy on a sandy estuarine beach. Journal of Sedimentary Petrology 63, 1152–1159.

Oakey, R., Green, M., Carling, P.A., Lee, M.W.E., Sear, D.A., Warburton, J., 2005. Grain-shape analysis — a new method for determining representative particle shapes for populations of natural grains. Journal of Sedimentary Research, 75, 1065–1073.

Osborne, P.D., 2005. Transport of gravel and cobble on a mixed sediment inner bank shoreline of a large inlet, Grays Harbor, Washington. Marine Geology 224, 145–156.

Osborne, P.D., Boak, E.H., 1999. Sediment suspension and morphological response under vessel-generated wave groups: Torpedo Bay, Auckland, New Zealand. Journal of Coastal Research 15 (2), 388–398.

Osborne, P.D., MacDonald, N.J., Reynolds, W.J., 2007. Response of mixed sediment beaches to wake wash from passenger only fast ferries: Rich Passage, Washington. In: McKee-Smith, Jane (Ed.), Proceedings of the 30th International Conference Coastal Engineering 2006. World Scientific, pp. 3105–3117.

Pacific International Engineering, 2007. Rich Passage Passenger Only Fast Ferry Study — Phase 2 Wave Energy Evaluation of Passenger Only Ferries in Rich Passage, Report 2. Integrated modeling of wake impacts, August 2007, prepared for FTA-WA-26-7007-2005. 205 pp.

Parnell, K.E., Kofoed-Hansen, H., 2001. Wakes from large high-speed ferries in confined coastal waters: management approaches with examples from New Zealand and Denmark. Coastal Management 29 (3), 217–237.

Parnell, K.E., Mc Donald, S.C., Burke, A.E., 2007. Shoreline effects of vessel wakes, Marlborough Sounds, New Zealand. Journal of Coastal Research 50 Special Issue.

Quick, M.C., Dyksterhuis, P., 1994. Cross-shore transport for beaches of mixed sand and gravel. International Symposium: Waves—Physical and Numerical Modeling. Canadian Society of Civil Engineers, pp. 1443–1452.

Rich Passage Wave Action Study Team, 2001. Rich Passage Wave Action Study, Monitoring Program Summary Report. Prepared for Washington State Ferries, August 2001.

Sneed, E.D., Folk, R.L., 1958. Pebbles in the Lower Colorado River, Texas: a study in particle morphogenesis. Journal of Geology 66, 114–150.

Soulsby, R.L., 1997. Dynamics of Marine Sands: A Manual for Practical Applications. Thomas Telford Publications.

Soulsby, R.L., Whitehouse, R.J.W., 1997. Threshold of sediment motion in coastal environments. Proc. Pacific Coasts and Ports '97 Conf., Christchurch, University of Canterbury, New Zealand, vol. 1, pp. 149–154.

Thomson, R.E., 1981. Oceanography of the British Columbia Coast. Canadian Special Publication of Fisheries and Aquatic Sciences 56. Department of Fisheries and Oceans.

Van Wellen, E., Chadwick, A.J., Mason, T., 2000. A review and assessment of longshore sediment transport equations for coarse grained beaches. Coastal Engineering 40, 243–275.

White, T.E., Inman, D.L., 1989. Transport determination by tracers: tracer theory. In: Seymour, R.J. (Ed.), Nearshore Sediment Transport. Plenum press, pp. 103–113.

Wilcock, P., Crowe, J., 2003. Surface-based transport model for mixed-size sediment. Journal of Hydraulic Engineering 120, 120–128.

Zingg, T., 1935. Beiträge zur Schotteranalyse. Schweizerische Mineralogische und Petrologische Mitteilungen, vol. 15, pp. 39–140.